

Laser-assisted collisions: The Kroll-Watson formula and bremsstrahlung theory

Sydney Geltman

JILA, University of Colorado and National Institute of Standards and Technology, Boulder, Colorado 80309-0440

(Received 25 September 1995)

Recent measurements on CO₂-laser-assisted electron-atom collisions have shown large inconsistencies with the Kroll-Watson formula for small-angle scattering. We have carried out a detailed study to compare the predictions of Kroll-Watson theory (for both single and multimode fields) with those of conventional perturbation theory for stimulated free-free transitions. It is found that for $E_0/2\omega^2 \ll 1$, where perturbation theory is valid, there are large differences with the Kroll-Watson theory. Comparisons of experimental variations with respect to scattering angle and electron energy show much better agreement with perturbation theory than with Kroll-Watson theory. A study of the angular variations in perturbation theory shows that use of the “outgoing” wave final state gives much better agreement with experiment than does the “ingoing” wave final state, which is different from the choice made in early bremsstrahlung theory. [S1050-2947(96)07405-7]

PACS number(s): 34.80.Qb, 03.65.Nk

I. INTRODUCTION

The free-free absorption and emission of radiation in electron-atom (and ion) collisions has been studied for 60 years as an important process in understanding stellar atmospheres and laboratory discharges and plasmas. With the availability of lasers it has become possible to make detailed differential cross beam studies of these cross sections, not only for single photon exchanges, but also as a multiphoton process. The major experimental effort in this work has been carried out by Weingartshofer, Wallbank, and co-workers over the past 20 years using a CO₂ laser and the scattering of low-energy electrons (~ 10 eV) by inert gas atoms (mainly He and Ar). The first measurement [1] taken at the large scattering angle of 153° and laser intensity of about 10^9 W/cm², clearly showed six peaks corresponding to the absorption and emission of up to three photons. Subsequent work [2–4] at $\sim 160^\circ$ at $\sim 10^8$ W/cm² revealed detectable peaks corresponding to the absorption and emission of up to 11 photons. Without presenting a detailed comparison of these results with the Kroll-Watson (KW) [5] formula, it was inferred that they were in qualitative agreement with it.

More recent measurements by Wallbank and Holmes [4,6,7] at small-angle scattering ($\sim 10^\circ$), however, revealed very serious disagreements with the Kroll-Watson formula. It was suggested that the effect of the polarization of the atom by the laser field, an effect not included in the KW formula, might account for these large discrepancies. Several authors [8–10] have made estimates of the effect of this additional atomic polarization and found that it would make much too small of a correction to the KW formula to account for the huge differences with experiment, which were as high as the order of 10^{15} for a five-photon process. A geometry for the free-free process, in which the laser polarization vector is adjusted to be perpendicular to the electron momentum change vector was also used by Wallbank and Holmes [7]. For this orientation the argument of the Bessel function that appears in the KW formula vanishes, and this would give a vanishing KW cross section for all ($n \neq 0$) photon exchanges. However, the measurements show very substantial cross sections, of the same order of magnitude as obtained

for other polarization directions. A useful review of all but the most recent work in this field is given by Mason [11].

These critical tests of the KW formula lead to the conclusion that it fails to agree with measurements over a wide range of conditions, and this has motivated the present study of it. The main objective of the present work is to compare KW theory in the weak-field limit with the earlier free-free transition theory which is based on the conventional perturbation theory (PT) treatment in powers of the intensity. In the following sections we will review Kroll-Watson theory in its single-mode and multimode forms, present a summary of the standard perturbation treatment of stimulated free-free transitions (also called “laser-assisted collisions”), use a model atom potential to evaluate free-free cross sections for one- and two-photon processes, and make overall comparisons among the two theoretical treatments (KW and PT) and the available experimental data. We will make these comparisons with respect to the variation of scattering angle, incident-electron energy, and laser intensity, and try to draw conclusions on the basis of the data available.

II. PRELIMINARY KINEMATICAL CONSIDERATIONS

If we consider a monoenergetic beam of electrons incident on a structureless target atom, only elastic scattering may take place in which $\mathbf{k}_i \rightarrow \mathbf{k}_f$ with the differential scattering cross section $d\sigma_{el}/d\Omega$, where $(d\sigma_{el}/d\Omega)d\Omega$ represents the electron flux scattered into $d\Omega$ divided by the incident electron flux density. We exclude such refinements as electron exchange or target atom excitations. When a laser field is applied, the electrons may also gain or lose energy in units of an integral number of photons while they undergo scattering. However, the laser itself cannot contribute to the scattering through any angle θ since it can only impart quiver motion to the electrons, but not change their overall directions. Thus if a scattered electron collector is placed at a scattering angle θ with acceptance angle $d\Omega$ and an energy spectrometer that would only admit electrons with energy $E_i \pm n\omega$, the electron flux it would record could be written as

$$\frac{d\sigma^{(n)}}{d\Omega} = \frac{k_f(n)}{k_i} P_n \frac{d\sigma_{\text{el}}}{d\Omega}, \quad (1)$$

where P_n is a probability that an n -photon transfer has taken place during the $\mathbf{k}_i \rightarrow \mathbf{k}_f$ scattering. In general P_n depends on all the parameters in the problem involving the electron, field, and atom. The requirement of particle conservation must apply to scattering by a potential that does not support any bound states (which we shall assume), and this is equivalent to the conservation of n -photon transfer probability, i.e.,

$$\sum_{n=-\infty}^{\infty} P_n = 1. \quad (2)$$

Generally the quantity that is measured in these experiments is the ratio of energy-selected electron flux into $d\Omega$ with the laser on to the purely elastically scattered electron flux into $d\Omega$ with the laser off. Thus these measured ratios would correspond to $(k_f(n)/k_i) P_n$ above. It will be the task of the dynamical theories we will consider in Secs. III and IV to predict the transition probabilities P_n as a function of all the physical variables.

III. KROLL-WATSON THEORY

The formula that we refer to as the Kroll-Watson formula [5] was also proposed in various forms by a number of other investigators [12–14], and has the form

$$\frac{d\sigma_{\text{KWSM}}^{(n)}}{d\Omega} = \frac{k_f(n)}{k_i} J_n^2(x) \frac{d\sigma_{\text{el}}(E_i, Q)}{d\Omega}. \quad (3)$$

Here $x = (\mathbf{E}_0/\omega^2) \cdot \mathbf{Q}$, the single-mode (SM) laser field is $\mathbf{E} = \mathbf{E}_0 \sin \omega t$, \mathbf{Q} is the momentum transfer $\mathbf{k}_i - \mathbf{k}_f(n)$, E_i is incident electron energy, and θ is the scattering angle. The Kroll-Watson derivation replaces E_i and Q by somewhat shifted values, but it has been shown that to a very good approximation these latter shifts are negligible in the low-frequency or soft-photon limit. (We use atomic units unless otherwise specified.) The CO_2 laser frequency corresponding to a photon energy of 0.117 eV or 0.00430 a.u. is expected to be small enough for this limit to apply.

The physical basis of the derivation of this formula arises from an S -matrix expansion for the scattering using Volkov basis states (free electron in the laser field), of which the first-order term is

$$S_{if}^{(1)} = -i \int_{-\infty}^{\infty} dt e^{-i(E_i - E_f)t} \int d\mathbf{r} e^{i\mathbf{k}_i \cdot [\mathbf{r} - \mathbf{r}_0(t)]} \times V(r) e^{-i\mathbf{k}_f \cdot [\mathbf{r} - \mathbf{r}_0(t)]}, \quad (4)$$

where $\mathbf{r}_0(t) = \alpha_0 \sin \omega t$, $\alpha_0 = \mathbf{E}_0/\omega^2$ is the classical amplitude of oscillation, and $V(r)$ is the atomic potential, assumed to be static. Making the Bessel function expansion

$$e^{ix \sin \omega t} = \sum_{n=-\infty}^{\infty} J_n(x) e^{in\omega t}, \quad (5)$$

carrying out the time integral in (4) and squaring to get the energy-conserving δ function, we see that to first order

$$\frac{d\sigma^{(n)}}{d\Omega} = \frac{k_f(n)}{k_i} J_n^2(x) \frac{d\sigma_{B1}(E_i, Q)}{d\Omega}, \quad (6)$$

where $d\sigma_{B1}/d\Omega$ is the first Born approximation for elastic scattering. Kroll and Watson, and others, have shown that the entire Born series can be formally summed in the low-frequency limit to give (3), where the exact elastic scattering cross section appears on the right-hand side.

The above result applies to the case of electron scattering in a single-mode laser field. This was later generalized to an extreme multimode or chaotic laser field [15,16], where it takes the form

$$\frac{d\sigma_{\text{KWMM}}^{(n)}}{d\Omega} = \frac{k_f(n)}{k_i} e^{-x^2/2} I_n(x^2/2) \frac{d\sigma_{\text{el}}(E_i, Q)}{d\Omega}, \quad (7)$$

where I_n are the modified Bessel functions of the first kind (approximately the ordinary Bessel functions of imaginary argument).

Note that both the single-mode and multimode (MM) forms of the KW formula have the property that the laser-on–laser-off ratio $(d\sigma_{\text{KW}}^{(n)}/d\Omega)/(d\sigma_{\text{el}}/d\Omega)$ are completely independent of the scattering atom, and only depend on laser properties and kinematic variables. Also we identify the transition probabilities P_n in (1) arising here as $J_n^2(x)$ and $e^{-x^2/2} I_n(x^2/2)$, and it is clear that the conservation condition (2) (often referred to as a sum rule) is satisfied by both of these forms for P_n in the $\omega \rightarrow 0$ limit. The details of the simultaneous interaction of the electron with the scattering potential and the laser field are factorized in this very clean way in Kroll-Watson theory, and thus it is not necessary to introduce any specific atomic model to evaluate these transition probabilities. All of the measurements are done in terms of the laser-on–laser-off ratio of cross sections, which is equivalent to $[k_f(n)/k_i] P_n$.

Kroll and Watson [5] state that their formula “provides a simple and reasonable approximation to multiphoton energy transfers when the frequency of the electromagnetic wave is small or when the scattering potential is weak.” One assumes that the “weakness of the scattering potential” means weak compared with the strength of the applied field, as would be understood by Eq. (4) being the first term in a perturbation expansion in $V(r)$. The CO_2 laser frequency is 0.00430 a.u. and the approximate weak electric field strength used in most of the measurements is 5×10^{-5} a.u. ($I \cong 10^8$ W/cm²). If we take the scattering potential to have the approximate magnitude of 1 a.u., then it certainly may not be considered as “weak” in this typical laser field, while the frequency may probably be regarded as sufficiently low. The question we seek to answer is whether the satisfying of only one of the two conditions is enough to expect the Kroll-Watson formula to be valid in the range of the current measurements.

IV. FREE-FREE TRANSITIONS IN PERTURBATION THEORY

Before the days of lasers the standard method for dealing with free-free transitions was the same perturbative method that applied to bound-bound (excitation) and bound-free (ionization) radiative processes. These of course are fully

discussed in the textbooks. The stimulated free-free process is clearly related to that of spontaneous bremsstrahlung, where an electron or other charged particle will emit photons when it is scattered, the analogue of classical charged particles emitting radiation when accelerated.

We seek the probability for a transition from one free state (\mathbf{k}_i) to another (\mathbf{k}_f) under the influence of a scattering potential $V(r)$ and an applied single-mode coherent field $\mathbf{E} = \mathbf{E}_0 \sin \omega t$. We take as basis states the full scattering wave functions $u_{\mathbf{k}}^{(+)}$, where the + represents the scattering boundary condition of an incident plane wave and outgoing scattered wave. We introduce the laser field at $t=0$, and seek a

perturbative solution to the time-dependent Schrödinger equation for $t > 0$, subject to the initial condition $\psi(\mathbf{r}, 0) = u_{\mathbf{k}_i}^{(+)}(\mathbf{r})$. We take the electron-field interaction to be $(1/\omega^2)\mathbf{E} \cdot \nabla V$, which is recognized as the ‘‘acceleration’’ form of the dipole interaction, and physically equivalent to the more common ‘‘length’’ form $\mathbf{E} \cdot \mathbf{r}$. The ‘‘acceleration’’ form is much more convenient to use in evaluating free-free matrix elements.

The twofold iteration of the integral equation form of the time-dependent Schrödinger equation leads to the second-order wave function

$$\begin{aligned} \psi^{(2)}(\mathbf{r}, t) = & u_{\mathbf{k}_i}^{(+)}(\mathbf{r}) e^{-iE_i t} - \sum_{\mathbf{k}} u_{\mathbf{k}}^{(+)}(\mathbf{r}) e^{-iE_k t} \left\{ \left(\frac{E_0}{2\omega^2} \right) M_{\mathbf{k}\mathbf{k}_i}^{(++)} \int_0^t dt' [e^{i(\omega_{\mathbf{k}\mathbf{k}_i} + \omega)t'} - e^{i(\omega_{\mathbf{k}\mathbf{k}_i} - \omega)t'}] \right. \\ & \left. + i \left(\frac{E_0}{2\omega^2} \right)^2 \sum_{\mathbf{k}'} M_{\mathbf{k}\mathbf{k}'}^{(++)} M_{\mathbf{k}'\mathbf{k}_i}^{(++)} \int_0^t dt' \left[\frac{e^{i(\omega_{\mathbf{k}\mathbf{k}_i} + 2\omega)t'}}{(\omega_{\mathbf{k}'\mathbf{k}_i} + \omega)} + \frac{e^{i(\omega_{\mathbf{k}\mathbf{k}_i} - 2\omega)t'}}{(\omega_{\mathbf{k}'\mathbf{k}_i} - \omega)} \right] \right\}, \end{aligned} \quad (8)$$

where $\omega_{\mathbf{k}\mathbf{k}'} = \frac{1}{2}(k^2 - k'^2)$ and $M_{\mathbf{k}\mathbf{k}'}^{(++)} = \int d\mathbf{r} u_{\mathbf{k}'}^{(+)*} (\hat{\mathbf{e}} \cdot \nabla V) u_{\mathbf{k}}^{(+)}$. This form retains only those terms corresponding to energy conservation (transient terms dropped). Each of the terms corresponding to one- and two-photon absorption and emission may be clearly identified. The transition amplitude to the final free state is obtained from the projection $\langle u_{\mathbf{k}_f}^{(+)} | \psi^{(2)} \rangle$, which when squared and summed over final states gives the transition probability. We have the following expressions for one- and two-photon absorption and emission effective cross sections:

$$\frac{d\sigma_{\text{PT}}^{(1)}}{d\Omega} = \frac{k_f}{(2\pi)^2} \left(\frac{E_0}{2\omega^2} \right)^2 |M_{\mathbf{k}_i\mathbf{k}_f}^{(++)}|^2,$$

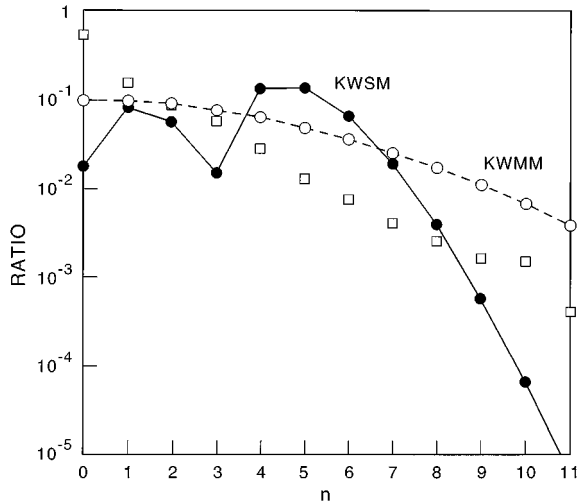


FIG. 1. Free-free transition laser-on-laser-off ratio for $\theta = 160^\circ$ and $\hat{\mathbf{e}} \parallel \mathbf{Q}$. Measurements [4] in Ar, at $E_i = 11.4$ eV and, $I = 1.3 \times 10^8$ W/cm², of average of absorption and emission of n photons (open squares). KW single mode (filled circles) and KW multimode (open circles).

$$\frac{d\sigma_{\text{PT}}^{(2)}}{d\Omega} = \frac{k_f}{(2\pi)^2} \left(\frac{E_0}{2\omega^2} \right)^4 \left| \sum_{\mathbf{k}} \frac{M_{\mathbf{k}_i\mathbf{k}}^{(++)} M_{\mathbf{k}\mathbf{k}_f}^{(++)}}{(\omega_{\mathbf{k}\mathbf{k}_i} \pm \omega)} \right|^2, \quad (9)$$

where in the intermediate state energy denominator the +, - signs go with two-photon absorption and emission, respectively. Any intermediate bound states would have to be included in the intermediate state sum.

At this point we introduce a specific typical model atom potential with which we may obtain numerical results. We choose

$$V(r) = -e^{-2r} \left(1 + \frac{1}{r} \right) - \frac{\alpha_p}{2} (1 - e^{-r})^6 / r^4, \quad (10)$$

which is a static field representation of a ground-state hydrogen atom, with polarizability $\alpha_p = 4.5$ a.u. This potential supports only one bound s state, which makes a negligible contribution to the sum in (9). The continuum basis states are expanded as

$$u_{\mathbf{k}}^{(+)}(\mathbf{r}) = \sum_{\ell=0}^{\infty} i^{\ell} (2\ell + 1) e^{i\eta_{\ell}(k)} \frac{v_{\ell}(r)}{kr} P_{\ell}(\hat{\mathbf{k}} \cdot \hat{\mathbf{r}}), \quad (11)$$

where the radial functions satisfy

$$\left[\frac{d^2}{dr^2} - \frac{\ell(\ell+1)}{r^2} - 2V + k^2 \right] v_{\ell}(r) = 0, \quad (12)$$

with asymptotic form beyond the range of V ,

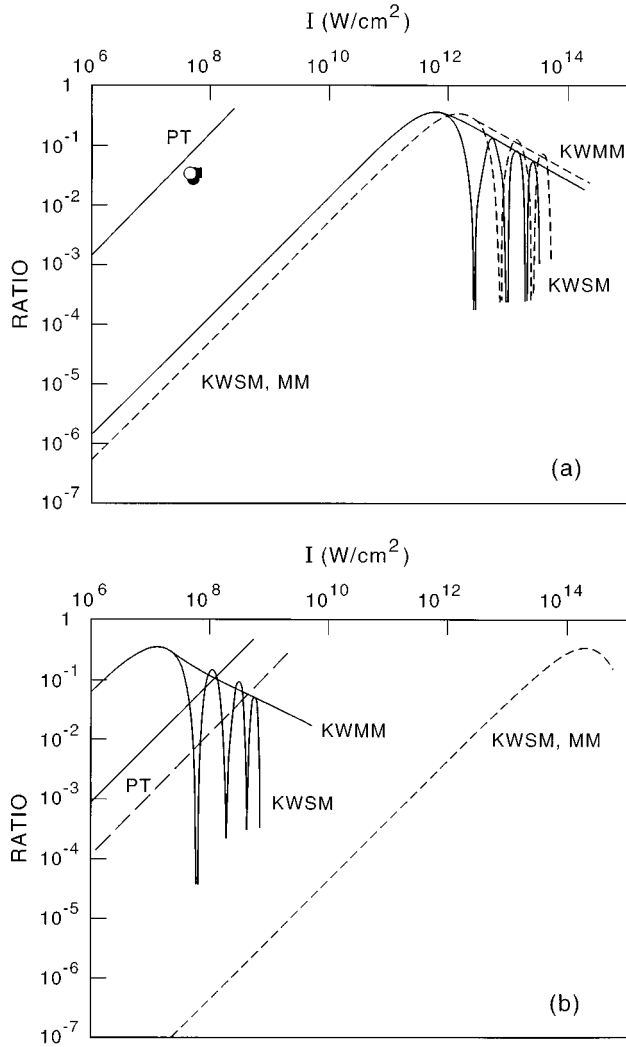


FIG. 2. Intensity dependence of free-free transition laser-on-laser-off ratio for one-photon absorption at $E_i = 10$ eV, and (a) $\theta = 10^\circ$ and (b) $\theta = 170^\circ$, polarization geometries G1 (solid lines) and G2 (dashed lines). KW single and multimode. PT results (G1 and G2 results coincide for $\theta = 10^\circ$). The points for $\theta = 10^\circ$ are from experiment [7] at $I = 0.52 \times 10^8$ W/cm 2 .

$$v_{\ell} \rightarrow kr[\cos \eta_{\ell} j_{\ell}(kr) - \sin \eta_{\ell} n_{\ell}(kr)], \quad (13)$$

which will eventually go to the form $\sin(kr - \frac{1}{2}\ell\pi + \eta_{\ell})$. After carrying out all angular integrals in (9) (shown in the Appendix), we are left with expressions in terms of the radial dipole matrix elements, in first order,

$$\mathcal{R}(\ell k, \ell' k') = \int_0^{\infty} dr v_{\ell} \frac{dV}{dr} v_{\ell'}, \quad (14)$$

and in second order

$$\mathcal{R}(\ell_i k_i \rightarrow \ell \rightarrow \ell_f k_f) = \int_0^{\infty} dk \frac{R(\ell_i k_i, \ell k) R(\ell k, \ell_f k_f)}{(k^2 - k_0^2)}, \quad (15)$$

where $k_0^2 = 2(E_i \pm \omega)$.

We solve (12) numerically with a Numerov procedure to obtain v_{ℓ} 's and η_{ℓ} 's and carry out numerical integrals for (14) and (15). The Cauchy principal value integral in (15) causes no problem, as a relatively small part of the total integral comes from the region of the pole. Since ω is so small, k_f and k_i are very close to one another and their corresponding η_{ℓ} 's are changed only slightly.

The perturbation theory cross sections obtained here are based on a single-mode laser field. The generalization to a multimode field has been obtained by Lambropoulos [17], and it results in an enhancement of the single-mode cross section by a factor of $n!$. This agrees with the enhancement factor in KW theory in the zero-intensity limit.

V. COMPARISON OF CALCULATED RESULTS

In this section we will present a detailed comparison of the results of the KW formulas with those of perturbation theory, and we will include comparisons with experiment

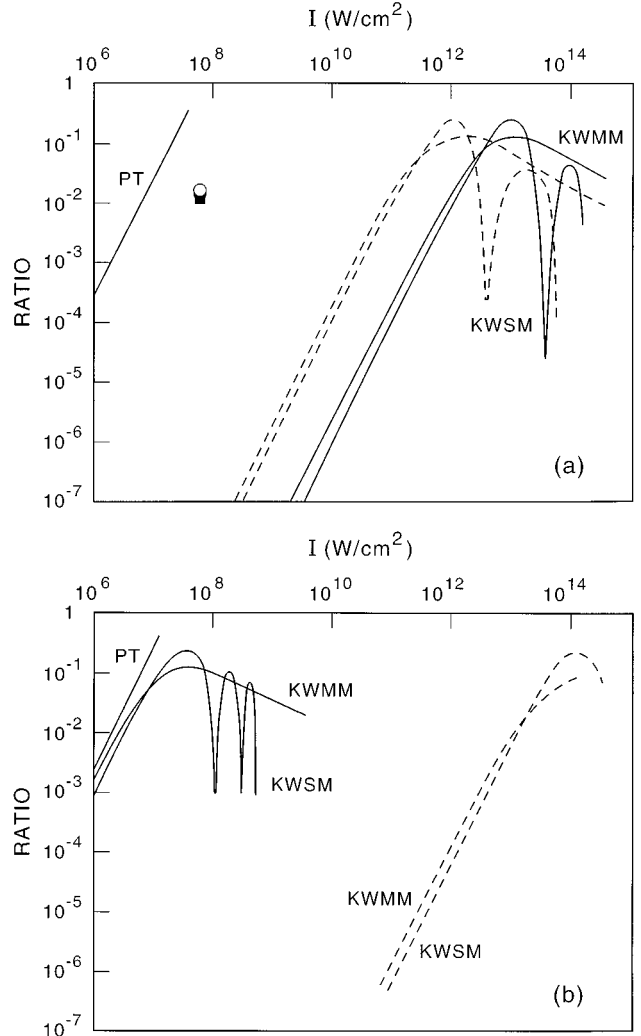


FIG. 3. Same for Fig. 2 but for two-photon absorption. The reversal of the expected limiting magnitudes of KW in G1 and G2 in (a) is the result of the fact that $\hat{\mathbf{e}} \cdot \mathbf{Q} = k_i - k_f \cos \theta$ in G1 is accidentally smaller than $\hat{\mathbf{e}} \cdot \mathbf{Q}$ in G2.

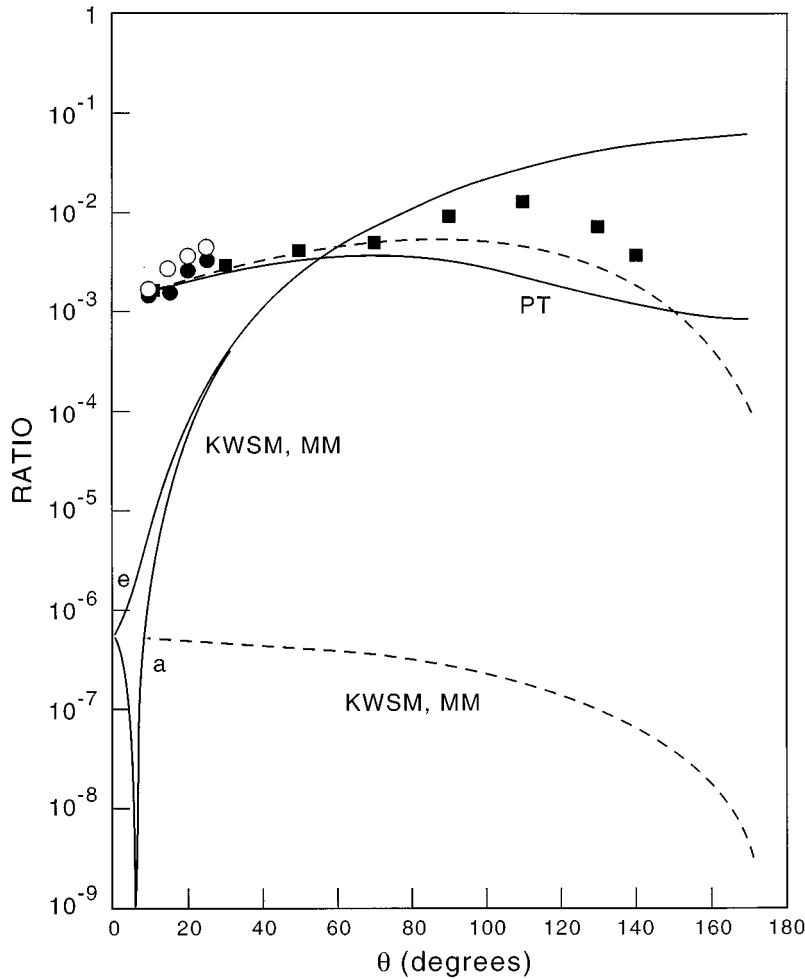


FIG. 4. Angular dependence of free-free transition laser-on-laser-off ratio for one-photon processes at $E_i = 10$ eV and $I = 10^6$ W/cm², polarization geometries G1 (solid lines) and G2 (dashed lines). The KW results in single and multimode coincide, and the differences in absorption and emission are indicated. The experimental points [7] measured at $\bar{I} = 0.52 \times 10^8$ W/cm² are for He (open circles) and Ar (filled circles) in G1, and for Ar (filled squares) in G2, and they have been fitted to the PT result at $\theta = 10^\circ$.

where possible. We start out with a look at the large-angle results, which have been studied most extensively experimentally [1–4], and which apparently give the best agreement with the KW theory. The most recent and exhaustive study by Wallbank and Holmes [4] on Ar was carried out at $\theta = 160^\circ$, $E_i = 11.4$ eV, $I \cong 1.3 \times 10^8$ W/cm², and with laser polarization vector $\hat{\epsilon}$ adjusted to be parallel to the momentum transfer vector \mathbf{Q} . This latter condition allows the magnitude of the argument of $J_n(x)$ to take its maximum value. Under these conditions they observed signals for the absorption and emission of up to 11 photons. In Fig. 1 we compare their measurements for the laser-on-laser-off ratio of $(d\sigma^{(n)}/d\Omega)/(d\sigma_{el}/d\Omega)$ for $n \geq 0$ (free-free absorption) with the calculated KW values for these conditions. We note that the agreement between the experimental points and the Kroll-Watson multimode formula is quite reasonable, in both shape and magnitude. It is remarkable that they are within an order of magnitude of each other over such a large range of photon numbers.

The recent experimental work [4,6,7] for small scattering angles, in which large discrepancies with KW theory have been found, has been carried out in two geometries for the laser polarization vector $\hat{\epsilon}$: G1: $\hat{\epsilon}$ parallel to $\hat{\mathbf{k}}_i$, the incident electron direction, and G2: $\hat{\epsilon}$ almost perpendicular to $\mathbf{Q} = \mathbf{k}_i - \mathbf{k}_f(n)$, the momentum transfer.

The latter geometry causes the arguments of the Bessel functions in both SM and MM forms of Kroll-Watson theory

to almost vanish, which would give very small predicted cross sections. It is thus a very critical probe of KW theory. The polarization vector is held fixed for all scattering angles in G1, but it is changed for every θ in G2 to maintain the condition $\hat{\epsilon} \cdot \mathbf{Q} \cong 0$.

In Figs. 2 and 3 we show the intensity dependence of the theoretical curves for one- and two-photon absorption. The corresponding curves for emission are omitted for the sake of clarity, and the only change expected would be a shift in the KW results for G1 at $\theta = 10^\circ$ of the magnitudes indicated in Figs. 4 and 5. The curves given are for small-angle (10°) and large-angle (170°) scattering. The striking feature of these curves is the large discrepancy in the low intensity limit between the KW and PT results. At the small angle PT is larger than KW by about 10^3 for $n = 1$ and by about 10^9 for $n = 2$, in both geometries. At the large angle the PT and KW are closer to one another in G1, but remain very far apart in G2. The relative closeness of the KW and PT results in G1 at the large scattering angles and lower intensities helps explain why the earlier measurements were found to be consistent with the KW formula. We note that the multimode version of KW removes the rapid oscillation that appears in the single-mode form, which arise from the $J_n^2(x)$ factor.

The experimental points given for $\theta \cong 10^\circ$ are those of Wallbank and Holmes [7] for average intensities in the first microsecond of their laser pulse, i.e., $\bar{I} = 0.52 \times 10^8$ W/cm²

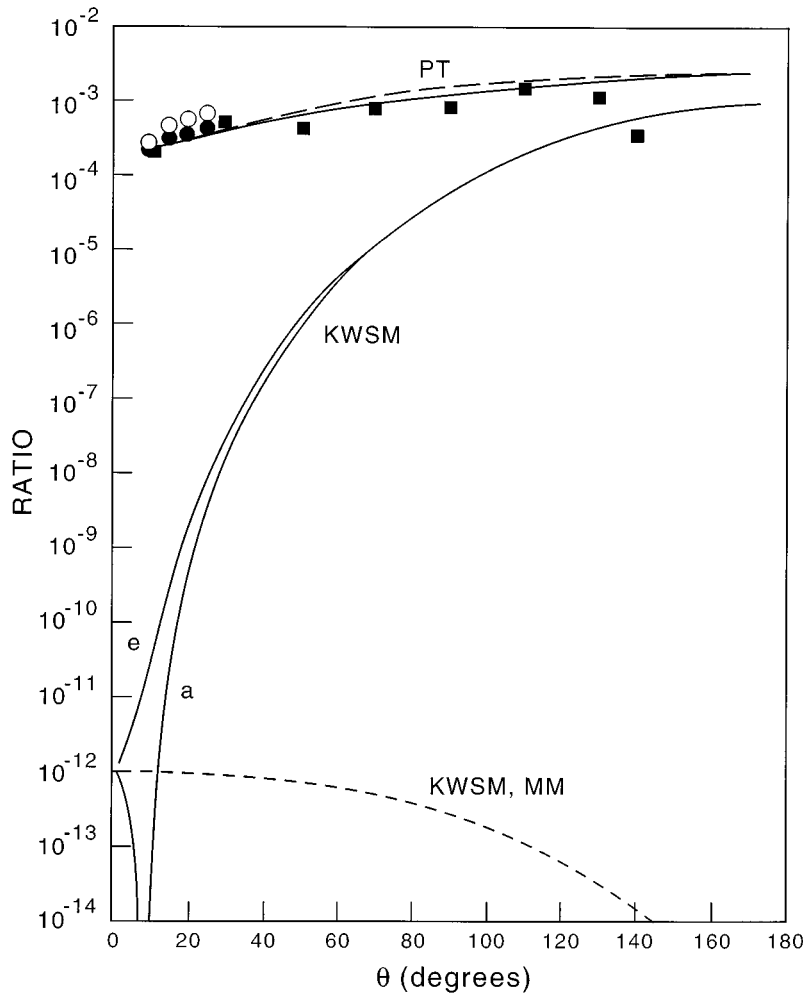


FIG. 5. Same for Fig. 4 but for two-photon processes. The theoretical curves shown are for single mode, and are enhanced by a factor of 2 in multimode.

for one-photon and $(\bar{I}^2)^{1/2} = 0.57 \times 10^8$ W/cm² for two-photon processes. We have also increased their measured ratios by a factor of 3 to approximately compensate for the fact that their electron beam is about 3 times wider than their laser beam. The resulting absolute measured points are seen to be reasonably consistent with our PT values, in the sense that the exact result might be expected to be given correctly by PT at $I = 10^6$ W/cm² ($E_0/2\omega^2 \cong 0.14$) from which it begins to bend over to approach the measured values at the experimental \bar{I} 's. The measured ratios appear to be near their maximum values since their values for the second microsecond of the pulse are of about the same magnitude as for the first microsecond, even though \bar{I} for the second microsecond has dropped to about 0.18×10^8 W/cm². On the other hand there appears to be no plausible joining that would make these measured values consistent with the KW curves. The higher orders of perturbation theory that would bring in the departures from the low-intensity limiting forms are prohibitive to carry out.

In Figs. 4 and 5 we show the angular dependence of one- and two-photon absorption and emission results in KW and PT at $I = 10^6$ W/cm² in the two polarization geometries along with measurements [7] in He and Ar taken at somewhat higher intensities. We normalize the data to the PT results at $\theta = 10^\circ$, which is consistent with our connection between the measured absolute values and PT calculations in

Figs. 2 and 3. We note the general overall agreement of the data with the PT results in both G1 and G2. The KW results in G1 show large divergences between absorption and emission at small angles. These are the result of a zero in $\hat{\mathbf{e}} \cdot \mathbf{Q} = k_i - k_f(n)\cos\theta$ for $k_f(n) > k_i$ (absorption) but not for $k_f(n) < k_i$ (emission). The almost total disappearance of the absorption component at small angles, as predicted by KW theory (single and multimode), has not been observed by Wallbank and Holmes (private communication) but rather they see almost equal contributions, as expected in PT.

In Figs. 6 and 7 are shown the cross-section ratios as a function of incident electron energy. At small scattering angle the large asymmetry between absorption and emission in the KW formula, which we saw in Figs. 4 and 5 for $E_i = 10$ eV, is seen to be present over a sizable energy range. The experimental points given in Figs. 6 and 7 were taken [4] in He at $\theta = 9^\circ$, and they correspond to an average of the n -photon absorption and emission signals. It is easy to see that the incident electron energy for which $k_i - k_f(n)\cos\theta = 0$ is given by $E_i = n\omega / [(1/\cos^2\theta) - 1]$, which for $n = 1$ and 2 and $\theta = 10^\circ$ is $E_i = 3.76$ and 7.53 eV, respectively. Again this extreme asymmetry in KW theory between absorption and emission was not seen in the measurements. On the other hand we see excellent agreement with the PT results, which are practically symmetric with respect to absorption and emission.

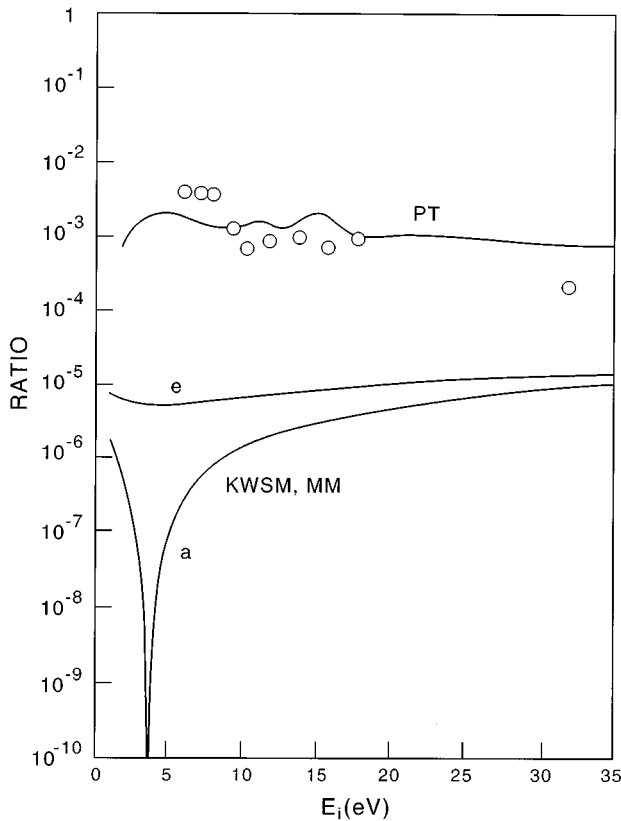


FIG. 6. Variation of free-free transition laser-on-laser-off ratio with incident electron energy for one-photon processes in polarization geometry G1 for $\theta=10^\circ$ and $\bar{I}=10^6$ W/cm 2 . KW absorption and emission as indicated. The experimental points [7] have been measured for He at $\theta=9^\circ$ and $\bar{I}=0.52 \times 10^8$ W/cm 2 , and have been fitted to the PT curve at $E_i=9.5$ eV.

VI. RELATION TO BREMSSTRAHLUNG THEORY

In the course of obtaining our present results in perturbation theory and relating this to conventional bremsstrahlung theory, we have come across an enigmatic question concerning the proper form to take for the final electron scattering state. In carrying out the time-dependent perturbation theory of Sec. IV we expanded in the complete set of eigenstates in the potential $V(r)$, which represented real scattering on that potential, i.e., the set $u_{\mathbf{k}}^{(+)}(\mathbf{r})$, having the “outgoing” wave form. In this way both the initial and final states $u_{\mathbf{k}_i}^{(+)}(\mathbf{r})$ and $u_{\mathbf{k}_f}^{(+)}(\mathbf{r})$ are members of this complete set. This naturally led to dipole matrix elements of the form

$$M_{\mathbf{k}_i, \mathbf{k}_f}^{(++)} \equiv \int d\mathbf{r} u_{\mathbf{k}_f}^{(+)*}(\hat{\mathbf{e}} \cdot \nabla V) u_{\mathbf{k}_i}^{(+)}, \quad (16)$$

in terms of which we have obtained all the PT results contained above.

The enigma lies in the fact that in the early work on bremsstrahlung [18], it has been emphasized that the final state should be taken to have “ingoing” wave form to give the matrix elements,

$$M_{\mathbf{k}_i, \mathbf{k}_f}^{(+-)} = \int d\mathbf{r} u_{\mathbf{k}_f}^{(-)*}(\hat{\mathbf{e}} \cdot \nabla V) u_{\mathbf{k}_i}^{(+)}, \quad (17)$$

a conclusion that was reached by general arguments involving time reversal.

The practical difference between the use of the two forms (16) and (17), as pointed out by Olsen [19], is only in regard to the differential cross sections for electron scattering, and the results become identical when integrated over $\hat{\mathbf{k}}_f$. This can be easily seen by referring to the expanded expression for $M_{\mathbf{k}_i, \mathbf{k}_f}^{(++)}$ in (A1). In this form of the matrix element the scattering phase shifts enter as $\exp[i\{\eta_{\ell}(k_i) - \eta_{\ell \pm 1}(k_f)\}]$, while in $M_{\mathbf{k}_i, \mathbf{k}_f}^{(+-)}$ the η 's are added rather than subtracted. This has the effect of changing the angular distribution, but not the total cross section, since one may verify that this factor goes out because of the orthogonality of the Legendre functions.

We show this effect in Figs. 8 and 9. We note that in G1 there is a crossing of the “outgoing” and “ingoing” PT results, so as to be consistent with the total free-free cross sections being identical with both forms of the final state. This situation is not present in G2 since that geometry involves a change of laser polarization with every change of scattering angle. For one-photon transfer in Fig. 8 we see that in G1 there is excellent agreement of the data with the “outgoing” form, while there is no sign of the sharp decrease at small angles predicted by the “ingoing” form. In G2 we see excellent agreement over a very wide angular range with the “outgoing” wave prediction. The fact that the

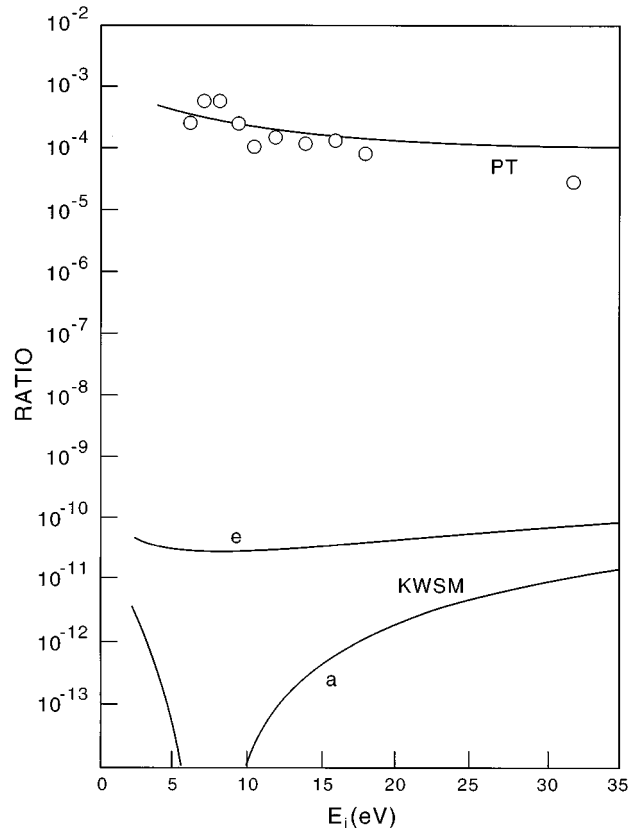


FIG. 7. Same for Fig. 6 but for two-photon processes in single mode. The multimode results are enhanced by a factor of 2 for both KW and PT.

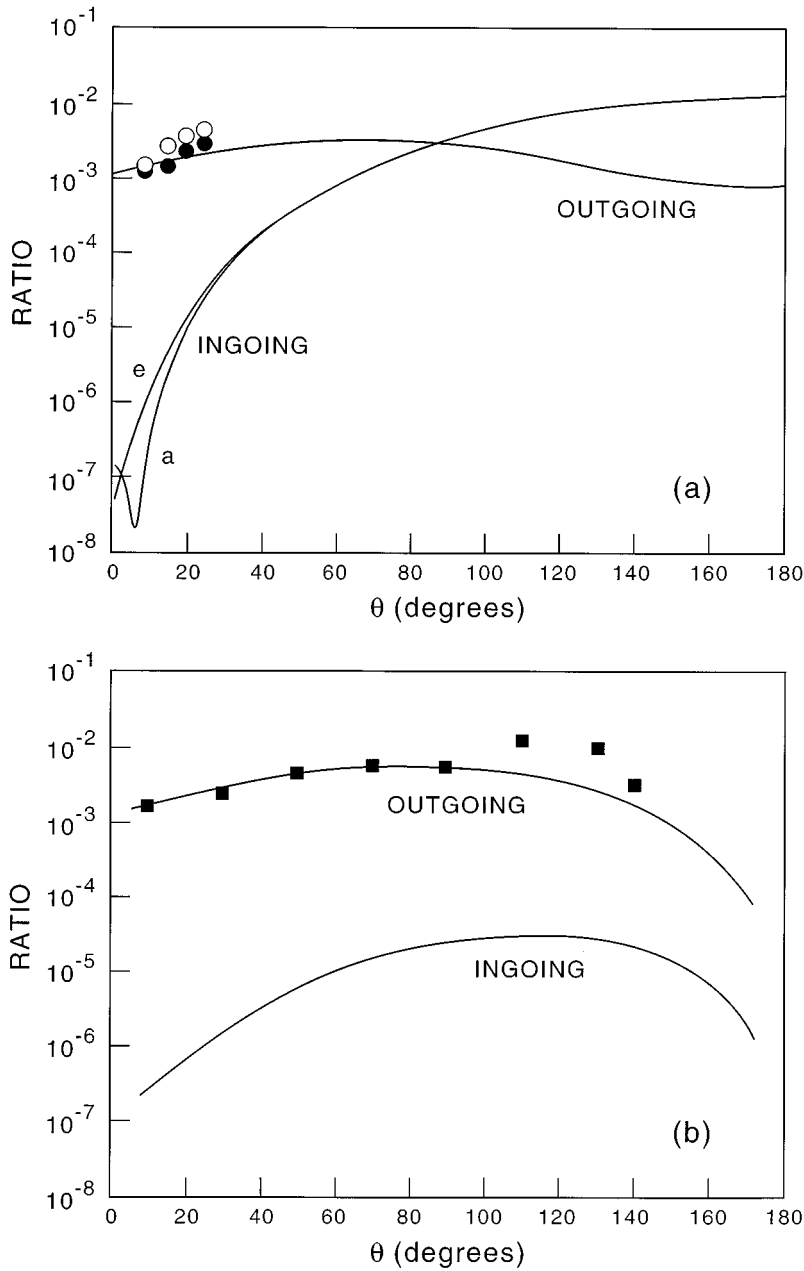


FIG. 8. Angular dependence of free-free transition laser-on-laser-off ratio as evaluated in PT using the “ingoing” and “outgoing” final state for one-photon processes at $E_i=10$ eV and $\bar{I}=10^6$ W/cm². These apply to both absorption and emission as indicated; (a) geometry G1 and (b) geometry G2. The experimental points are for measurements at $\bar{I}=0.52 \times 10^8$ W/cm² and have been fitted to the “outgoing” final-state results at $\theta=10^\circ$; He (open circles) and Ar (filled circles) at $E_i=10.5$ eV, and Ar (filled squares) at $E_i=10$ eV.

“ingoing” wave curve is so far below in absolute value also disagrees with the approximate absolute values of the data. For the two-photon results in Fig. 9 we find very little difference between the two theoretical results, unlike in the one-photon case, and there is certainly no preferred one insofar as an agreement with the data is concerned.

Most experimental work on high-energy bremsstrahlung involves the detection of the emitted photons as a function of angle and polarization. We are unable to find any measurements that are differential in the scattered charged particle, which would be necessary for a test of “ingoing” versus “outgoing” wave final states. It appears that the first such detailed studies are the presently considered electron-atom stimulated free-free transitions, and that these measurements strongly favor the “outgoing” wave final state.

The Low theorem [20] relates the “ingoing” wave dipole matrix element $M_{\mathbf{k}_i\mathbf{k}_f}^{(+)}$ to elastic scattering amplitudes in the $\omega \rightarrow 0$ limit, and has the nonrelativistic form

$$M_{\mathbf{k}_i\mathbf{k}_f}^{(+)} \sim \frac{1}{\omega} \hat{\mathbf{e}} \cdot (\mathbf{k}_i - \mathbf{k}_f) f(\bar{E}, Q) + \frac{1}{2} \hat{\mathbf{e}} \cdot (\mathbf{k}_i + \mathbf{k}_f) \frac{\partial f(E_i, Q)}{\partial E_i}, \quad (18)$$

where $\bar{E} = \frac{1}{2}(E_i + E_f)$. The sharp dip in Fig. 8(a) at $\theta \cong 6^\circ$ in the result for an “ingoing” final state appears to correspond to $\hat{\mathbf{e}} \cdot (\mathbf{k}_i - \mathbf{k}_f) = 0$ for a one-photon absorption, which also gave the zero at that angle in the KW result in Fig. 4. There is also a large asymmetry between absorption and emission in that angular region for the KW formula as there is using $M_{\mathbf{k}_i\mathbf{k}_f}^{(+)}$ in perturbation theory. The resemblance between the “ingoing” wave PT results in Fig. 8 and the KW results in Fig. 4, in both polarization geometries, suggests that the KW derivation is based on the use of an “ingoing” wave final state. One could speculate on the basis of this that a “KW-type” derivation that was based on an “outgoing” wave

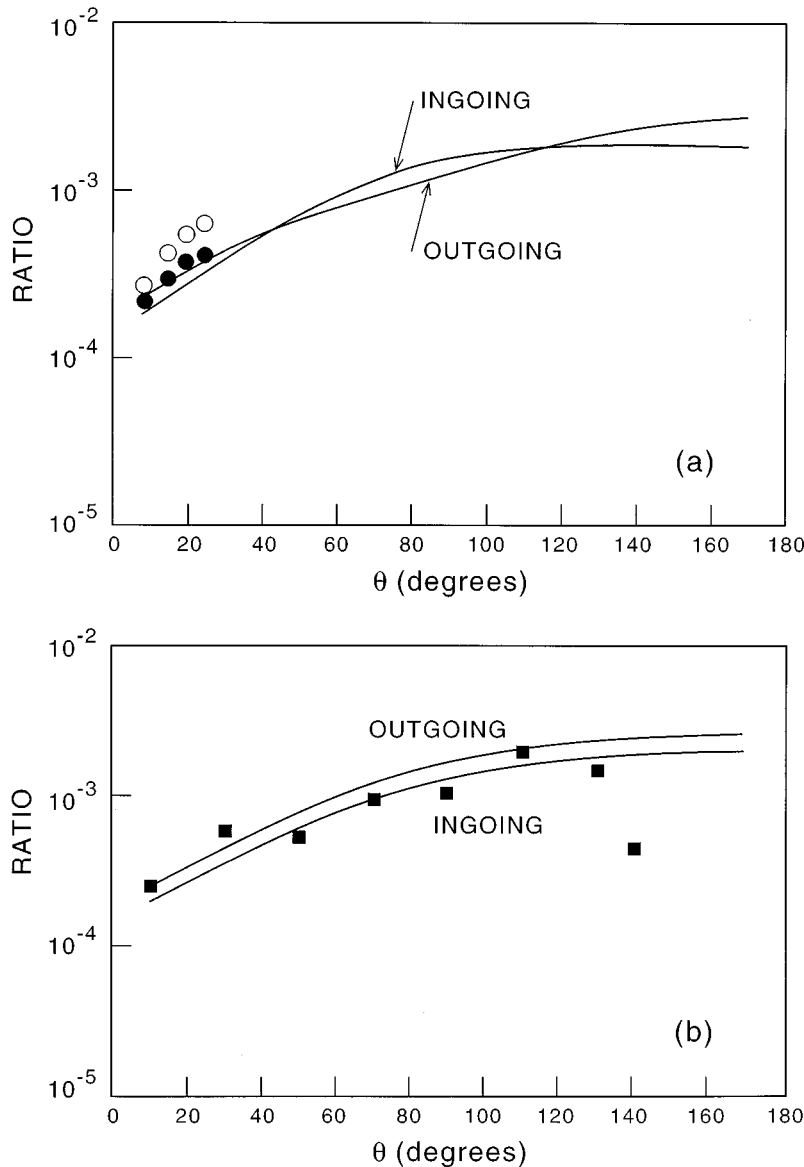


FIG. 9. Same for Fig. 8 but for two-photon single-mode process. The multimode results are enhanced by a factor of 2.

final state might result in better agreement with experiment than is obtainable with the present KW formulas.

We might also expect that in the high electron energy limit, where the Born approximation becomes exact and all $\eta_{\ell} \rightarrow 0$, the differences between using the “ingoing” and “outgoing” final states in perturbation theory will disappear. This is the result of the fact that these differences arise from the $\exp[i\{\eta_{\ell}(k_i) \pm \eta_{\ell}(k_f)\}]$ factors in the partial wave expansion for the dipole matrix element (see the Appendix). The application of the Low theorem in that limit would also imply a confluence of these two PT results with the KW result.

We are unable to see how the use of an “ingoing” wave final state could be consistent with our perturbation expansion in Sec. IV. We believe it is essential to expand the time-dependent wave function in a complete, orthonormal set of stationary states, and that this could not be achieved by mixing $u_{\mathbf{k}}^{(-)}$ states in with our basis of $u_{\mathbf{k}}^{(+)}$ states. It seems that to obtain a physically meaningful transition amplitude, both the initial and final states should be part of the same

basis set used for the expansion of the exact wave function. This is a point that deserves much further investigation.

VII. SUMMARY AND CONCLUSIONS

We have carried out a critical study on the validity of Kroll-Watson theory in low-energy electron-atom free-free transitions in the presence of CO_2 laser radiation, which was motivated by very large differences between its predictions and laboratory measurements, particularly for small-angle scattering. We have made detailed calculations of the ratio of laser-on–laser-off signals for one- and two-photon transfer differential in scattering angle, both in KW theory and perturbation theory (stimulated bremsstrahlung), and compared these with the available experimental data. This ratio is independent of target atom in KW theory but not in PT, so a typical atomic potential was used for the latter calculations.

It is found that in all comparisons made, including the variations with respect to scattering angle and incident electron energy (at fixed laser intensity) the agreement with experiment is far better with PT than with KW. There are also

large differences between KW and PT predictions in the low-intensity limit, where PT is expected to be valid. The effects of multimode structure in the laser pulse is compared with single mode and its main effect in KW theory is to smooth out the high-intensity oscillations arising from the $J_n^2(x)$ factor. In general we support the conclusions of Wallbank and Holmes that KW theory is grossly inadequate to describe small-angle free-free transitions stimulated by CO₂ laser radiation.

An interesting theoretical outcome of the perturbation theory calculations is that the “outgoing” wave final state was found to give much better agreement with the differential cross section measurements than is obtained using the “ingoing” wave final state. This is opposite to what is expected on the basis of bremsstrahlung theory, where the “ingoing” wave final state was felt to be the correct form. They both give the same integrated cross section, which is the quantity generally measured in the older bremsstrahlung experiments. Thus the recent laser-assisted electron scattering

measurements appear to be the most detailed experimental test of this theoretical question.

ACKNOWLEDGMENTS

I am extremely indebted to Barry Wallbank for his helpful cooperation in providing me with the experimental data in tabular form and for many useful discussions on the measurements. I have also had helpful discussions on theoretical questions with Leonard Maximon, Edward Robinson, and Leonard Rosenberg.

APPENDIX

We present here the detailed partial-wave forms for the PT first- and second-order matrix elements, which appear in (9):

$$M_{\mathbf{k}_i \mathbf{k}_f}^{(++)} = i \frac{(4\pi)^2}{k_i k_f} \sum_{\ell=0}^{\infty} (2\ell+1)^{1/2} e^{i\eta_{\ell}(k_i)} \left\{ e^{-i\eta_{\ell-1}(k_f)} (2\ell-1)^{-1/2} C(\ell 1 \ell-1; 000) R(\ell k_i, \ell-1 k_f) \right. \\ \times \sum_m Y_{\ell m}(\hat{\mathbf{k}}_i) Y_{\ell-1 m}^*(\hat{\mathbf{k}}_f) C(\ell 1 \ell-1; m 0 m) - e^{-i\eta_{\ell+1}(k_f)} (2\ell+3)^{-1/2} C(\ell 1 \ell+1; 000) R(\ell k_i, \ell+1 k_f) \\ \left. \times \sum_m Y_{\ell m}(\hat{\mathbf{k}}_i) Y_{\ell+1 m}^*(\hat{\mathbf{k}}_f) C(\ell 1 \ell+1; m 0 m) \right\} \quad (\text{A1})$$

$$\sum_{\mathbf{k}} \frac{M_{\mathbf{k}_i \mathbf{k}}^{(++)} M_{\mathbf{k} \mathbf{k}_f}^{(++)}}{(\omega_{k k_i \pm \omega})} = - \frac{64\pi}{k_i k_f} \sum_{\ell=0}^{\infty} (2\ell+1)^{1/2} e^{i\eta_{\ell}(k_i)} \{ C(\ell 1 \ell-1; 000) [e^{-i\eta_{\ell-2}(k_f)} (2\ell-3)^{-1/2} C(\ell-1 1 \ell-2; 000) \\ \times A_{\ell} \mathcal{R}(\ell k_i \rightarrow \ell-1 \rightarrow \ell-2 k_f) - e^{-i\eta_{\ell}(k_f)} (2\ell+1)^{-1/2} C(\ell-1 1 \ell; 000) \\ \times B_{\ell} \mathcal{R}(\ell k_i \rightarrow \ell-1 \rightarrow \ell k_f)] - C(\ell 1 \ell+1; 000) [e^{-i\eta_{\ell}(k_f)} (2\ell+1)^{-1/2} C(\ell+1 1 \ell; 000) \\ \times C_{\ell} \mathcal{R}(\ell k_i \rightarrow \ell+1 \rightarrow \ell k_f) - e^{-i\eta_{\ell+2}(k_f)} (2\ell+5)^{-1/2} C(\ell+1 1 \ell+2; 000) \\ \times D_{\ell} \mathcal{R}(\ell k_i \rightarrow \ell+1 \rightarrow \ell+2 k_f)] \}, \quad (\text{A2})$$

where the radial factors R and \mathcal{R} are defined in (14) and (15), and the angular factors are

$$A_{\ell} = \sum_m Y_{\ell m}(\hat{\mathbf{k}}_i) Y_{\ell-2 m}^*(\hat{\mathbf{k}}_f) C(\ell 1 \ell-1; m 0 m) \\ \times C(\ell-1 1 \ell-2; m 0 m),$$

$$B_{\ell} = \sum_m Y_{\ell m}(\hat{\mathbf{k}}_i) Y_{\ell m}^*(\hat{\mathbf{k}}_f) C(\ell 1 \ell-1; m 0 m) \\ \times C(\ell-1 1 \ell; m 0 m),$$

$$C_{\ell} = \sum_m Y_{\ell m}(\hat{\mathbf{k}}_i) Y_{\ell m}^*(\hat{\mathbf{k}}_f) C(\ell 1 \ell+1; m 0 m) \\ \times C(\ell+1 1 \ell; m 0 m),$$

$$D_{\ell} = \sum_m Y_{\ell m}(\hat{\mathbf{k}}_i) Y_{\ell+2 m}^*(\hat{\mathbf{k}}_f) C(\ell 1 \ell+1; m 0 m) \\ \times C(\ell+1 1 \ell+2; m 0 m).$$

All spherical harmonics above are expressed in terms of the polar axis taken along $\hat{\mathbf{e}}$, the field polarization direction. The above forms correspond to taking the “outgoing” wave modification of the final state. The corresponding forms for the “ingoing” wave modification would require the replacement of all $e^{-i\eta_{\ell}(k_f)}$ by $e^{i\eta_{\ell}(k_f)}$.

- [1] A. Weingartshofer, J. K. Holmes, G. Caudle, E. M. Clarke, and H. Krüger, *Phys. Rev. Lett.* **39**, 269 (1977).
- [2] A. Weingartshofer, E. M. Clarke, J. K. Holmes, and C. Jung, *Phys. Rev. A* **19**, 2371 (1979).
- [3] A. Weingartshofer, J. K. Holmes, J. Sabbagh, and S. L. Chin, *J. Phys. B* **16**, 1805 (1983).
- [4] B. Wallbank and J. K. Holmes, *J. Phys. B* **27**, 1221 (1994).
- [5] N. M. Kroll and K. M. Watson, *Phys. Rev. A* **8**, 804 (1973).
- [6] B. Wallbank and J. K. Holmes, *Phys. Rev. A* **48**, R2515 (1993).
- [7] B. Wallbank and J. K. Holmes, *J. Phys. B* **27**, 5405 (1994).
- [8] J. Rabadán, L. Mendez, and A. S. Dickinson, *J. Phys. B* **27**, L5535 (1994).
- [9] S. Geltman, *Phys. Rev. A* **51**, R34 (1995).
- [10] S. Varró and F. Ehlötzky, *Phys. Lett. A* **203**, 203 (1995).
- [11] N. J. Mason, *Rep. Prog. Phys.* **56**, 1275 (1993).
- [12] F. V. Bunkin and M. V. Federov, *Zh. Éksp. Teor. Fiz.* **49**, 1215 (1965) [*Sov. Phys. JETP* **22**, 844 (1966)].
- [13] H. Krüger and C. Jung, *Phys. Rev. A* **17**, 1706 (1978).
- [14] L. Rosenberg, *Phys. Rev. A* **20**, 275 (1979); **21**, 1939 (1980); **23**, 2283 (1981).
- [15] P. Zoller, *J. Phys. B* **13**, L249 (1980).
- [16] R. Daniele and G. Ferrante, *J. Phys. B* **14**, L635 (1981).
- [17] P. Lambropoulos, *Advances in Atomic and Molecular Physics* (Academic, New York, 1976), Vol. 12, p. 87.
- [18] See, for example, H. A. Bethe, F. E. Low, and L. C. Maximon, *Phys. Rev.* **91**, 417 (1953); G. Breit and H. A. Bethe, *ibid.* **93**, 888 (1954).
- [19] H. Olsen, *Phys. Rev.* **99**, 1335 (1955).
- [20] F. E. Low, *Phys. Rev.* **110**, 974 (1958).